

T.G. Edossa¹, M.M. Woldemariam²

Electronic, Structural and Optical Properties of Zincblend and Wurtizite Cadmium Selenide (CdSe) Using Density Functional Theory and Hubbard Correction

¹College of Natural and Computational science, Wollega University, Wollega, Ethiopia. teshgerb@gmail.com

²College of Natural Sciences, Jimma University, Jimma, Ethiopia, menberu.mengesha@ju.edu.et

Zinc blende (ZB) and wurtzite (WZ) structure of cadmium selenide (CdSe) is determined using density-functional theory within local density approximation (LDA), generalized gradient approximation (GGA), Hubbard-correction (GGA + U) and Hybrid functional approximation (PBE0 or HSE06). The convergence test of total energy with respect to cutoff energy and k-point sampling is performed to assure the accuracy of calculation. The equilibrium lattice constant of CdSe in both phases are calculated and the obtained values are in good agreement with experimental values. The calculated band gap values of CdSe in WZ and ZB phase are severely underestimated. However, the band gap values obtained by using GGA + U and the hybrid functional approximations are consistent with the experimental results. Optical properties: complex and real parts of dielectric function, energy loss spectrum and absorption coefficient of CdSe in both ZB and WZ phase were studied. The calculated static dielectric constant $\epsilon_1(0)$ of ZB CdSe is 11.7595, 13.7050 and 8.2099 for LDA, PBE and DFT + U approximations respectively. The value obtained using Hubbard correction is consistent with the experimental result. Moreover, the static dielectric constant $\epsilon_1(0)$ of WZ CdSe is 8.1211, 5.3536 and 4.2133 for LDA, PBE and DFT + U approximations in that order. The optical absorption spectrums of both phases have several peaks which correspond to different electronic transitions from occupied to unoccupied band. However, the loss function describes the loss of energy while traversing through the material.

Key words: Cadmium Selenide, DFT, equilibrium lattice constant, band structure, optical properties.

Received 31 October 2020; Accepted 15 December 2020.

Introduction

Cadmium selenide (CdSe) is a semiconductor compound of the II-VI family which crystalizes in zinc blend and wurtzite phases [1]. CdSe is transparent in the infrared region of the electromagnetic spectrum [2]. It has high efficiency of radiative recombination, high absorption coefficient and high photosensitivity [3-6]. - CdSe has been extensively studied due to its technological applications such as light-emitting diodes [7-9], solar cells, photodetectors and optoelectronic [10, 11] and photovoltaic devices [12, 13]. ZB- CdSe is a stable phase at low temperature and transform to wurtzite structure above critical temperature [14]. The electronic and structural properties of CdSe are studied using LDA [15]. The electronic band structure of CdSe is studied by angle

resolved photoemission [16]. The elastic, electronic and lattice dynamical properties CdSe is studied using LDA [17]. In addition to this the band gap of CdSe is calculated using EV-GGA [18]. However, these LDA based computational results of the band gap are found to be lower than the experimental band gap values. Even though, EV-GGA method improves the band gap value, it also underestimates the band gap value in comparisons to the experimental band gap values. In present study the electronic, structural and optical properties of ZB- and WZ- phase of CdSe are determined using LDA, GGA, GGA + U and PBE0 methods. The article is organized as follows: Section 2 describes the method of calculation. Moreover, the results and discussion are presented in section 3. Finally the findings are concluded in section 4.

Table 1

Crystal structure data is compared with both theoretical and experimental data.							
Methods		LDA			PBE	DFT+U	PBE0
ZB	Present	a = 6.082			a = 6.214	a = 6.220	a = 6.082
	Theories	a = 6.305[34], 6.239[33], 6.05[35]					
	Experiment	a = 6.084[36]					
WZ	Present	a = 4.253			a = 4.385	a = 4.417	a = 4.253
		c = 6.920, u=0.373			c = 6.863 u = 0.374	c = 7.186 u=0.376	c = 6.920 u = 0.374
	Theories	a=4.390[33]	a=4.20[36]				
		c=7.10	c=6.80				
	Experiment	a = 4.310[33]					
	c = 7.010						

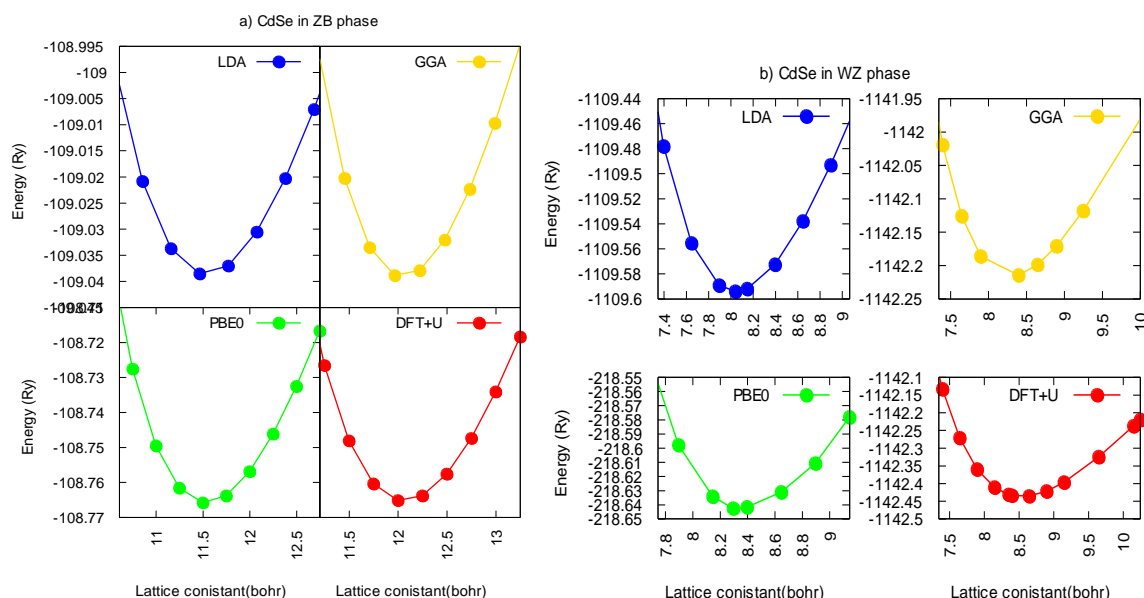


Fig. 1. Lattice constant versus total energy of CdSe: a) ZB b) WZ Phases.

I. Computational methods

Many body problems are very difficult to solve [19]. That is, the state of motion cannot be solved analytically for systems in which three or more distinct electrons interact [20]. Density functional theory is emerged for such problems [21-23]. In this article the calculations are performed using Quantum-ESPRESSO (QE) package that is based on DFT and plane wave pseudo potential method [24, 25]. In Khon Sham equations, the exchange correlation potential is difficult to predict and a puzzling term in DFT. To estimate this potential LDA [26], PBE [27], GGA + U [28] and hybrid (PBE0) [29] functional are implemented. The pseudopotentials developed for QE package (PBE QE UPF, LDA QE UPF and PBESOL QE UPF) from the GBRV Pseudopotential library [30] and PAW pseudopotentials [31] are implemented in the potential approximation. While approximating this potential the core electrons which cannot participate in the chemical bonding of the system are frozen and only valence electrons are considered. The electron configuration of cadmium is [Kr] 4d¹⁰5s² and that of selenium is [Ar] 3d¹⁰4s²4p⁴. In order to treat the strong

electron-electron correlation among the d-electrons of the system the Hubbard correction is introduced. The optimal Hubbard parameter U used for ZB and WZ CdSe are 3.0 and 3.4 eV respectively. Moreover, the value of mixing parameter in the hybrid function PBE0 is 0.25. For convergence tests, the electronic wave functions are expanded in a plane wave basis set with trial cut-off energy. The k-point sampling of the Brillion zone is constructed using Monk Horst Pack Mesh scheme [32]. The convergence test for total minimum energy as a function of cutoff energy is performed with an increment of 10 Ry in the range of 10 to 100 Ry. While varying the energy cutoff the other parameters in the input file made fixed. For good total minimum energy convergence we have used the criteria that the change in energy (ΔE) from the reference point (100 Ry) to be approximately equal to 4×10^{-4} Ry per cell. In this calculation, $\Delta E = 3.8 \times 10^{-4}$ per cell (9.5×10^{-5} Ry per atom) for WZ- CdSe at 55 Ry energy cutoffs for LDA approximation and less than this value for GGA, PBE0 and GGA + U approximations. Moreover, $\Delta E = 1.65 \times 10^{-4}$ per cell (8.25×10^{-5} Ry per atom) for ZB CdSe at 60 Ry energy cutoffs for LDA approximation, and less than this value for other types of approximations.

Similarly the convergence test for total minimum energy versus k -point sampling with an increment of $2 \times 2 \times 2$ from the range of $2 \times 2 \times 2$ to $10 \times 10 \times 10$ is performed fixing the other parameters constant. It is observed that a $6 \times 6 \times 6$ k -point samplings for Brillion zone integration yield accurately converged total energy of ZB-CdSe for LDA, PBE, DFT+U and PBE0 respectively. In case of WZ-CdSe the total energy converged at $7 \times 7 \times 7$ k -point sampling for Brillion zone integration in relation to LDA, PBE, PBE0 and DFT + U. Using the values of cutoff energy and k -point sampling from the energy convergence calculation, the structural optimization was done by giving initial lattice constant (a_0) smaller than the expected value in the calculation of total energy. The calculations are iterated where at the end of each step we obtained a new structural parameter (a) and the new total energy (E). The iteration continued until we obtain the lowest total energy.

II. Results and discussion

2.1 Equilibrium Lattice Constant

The equilibrium lattice constants of CdSe in ZB and WZ phases are calculated using plane wave self-consistent field (PWSCF). In this calculation, the cutoff energy and k -point sampling are the points at which the total energy is converged. The calculated values of lattice parameters using LDA, PBE, DFT+U and PBE0 methods are shown in Table 1 and compared with previous theoretical and experimental results. Moreover, the value of structural parameter for WZ CdSe is the nearest neighbor distance along c -axis in units of c . Its value for ideal WZ CdSe structure is 0.375. It shows that our calculations in accord with LDA, PBE, DFT + U and PBE0 are in good agreement with previous theoretical and experimental results. LDA underestimates the lattice constant by 1 % whereas PBE overestimates it. Moreover, lattice constant versus total energy is displayed in Fig. 1.

2.2 Electronic properties of CdSe

The band-gap and band structures along high symmetry points of Brillouin zone of CdSe in ZB and WZ structure are performed within LDA, GGA, GGA + U and PBE0 potential approximations. The calculated electronic band structures within LDA, GGA, DFT+U and PBE0 are shown in 2a for ZB-CdSe and 2b for WZ-CdSe phase. The band structure shows that CdSe in both ZB and WZ phase is a direct band gap semiconductor as the top valence and bottom conduction bands aligned at the same high symmetry Γ point. Moreover, the calculated band-gap in electron volt (eV) is summarized in Table 2 and compared with the experimental result.

LDA and GGA potential approximations severely underestimate the band gap values of CdSe in ZB and WZ phase. This problem was improved by using projector augmented-wave pseudopotential within Hubbard-correction (GGA + U) and hybrid functional approximation (PBE0) [37-40]. The band gap values obtained by using GGA + U and hybrid functional approximations are in good agreement with the experimental band gap values.

Density of state for ZB- and WZ-CdSe is determined

within LDA, PBE and DFT+U as demonstrated in Fig. 3a and 3b. Density of states (DOS) describes the behavior of states occupancy over specific energy level. It gives a detail of the states which are unoccupied and the states which are occupied. A high DOS at a specific energy level describe the states available for occupation. For both phases the density of states are discontinuous for the width from the top of valence band to the bottom of conduction band which is normally the band gap of the system.

2.3 Optical properties of CdSe

An investigation of optical properties of CdSe is very essential for optoelectronic applications. So the fundamental quantities, frequency dependent complex dielectric function were calculated. Complex dielectric function is the combination of the imaginary $\epsilon_2(\omega)$ and real $\epsilon_1(\omega)$ parts of the permittivity. WZ CdSe crystal structure is anisotropic and has the perpendicular and parallel components of polarization. However, in this article we considered a monochromatic laser source of light is applied parallel to the c -axis and considered only the parallel component of the polarization and the dielectric function related to this polarization. Other optical properties such as absorption coefficient, extinction coefficient, energy loss and refractive index are acquired from these fundamental quantities. The frequency dependent imaginary dielectric function $\epsilon_2(\omega)$ of materials [31] is given by equation:

$$\epsilon_2(\omega) = \frac{8}{2\pi\omega^2} \sum_{nn'} \int_{BZ} |P_{nn'}(k)|^2 \frac{dS_k}{\nabla\omega_{nn'}(k)} \quad (1)$$

Where \int_{BZ} is an integration over the entire Brillouin zone, $\sum_{nn'}$ is the sum over all initial valence band and final conduction band states, $|P_{nn'}(k)|^2$ is the dipole matrix element between final and initial states, dS_k is energy surface with constant value, $\omega_{nn'}(k)$ is the energy difference between two states. The real part of dielectric function $\epsilon_1(\omega)$ can be extracted from imaginary part using Kramer-Kroning relation [42].

$$\epsilon_1(\omega) = 1 + \frac{2}{\pi} P \int_0^\infty \frac{\omega' \epsilon_2(\omega')}{\omega'^2 - \omega^2} d\omega', \quad (2)$$

where P is the principal value of the integral.

Hence the frequency dependent imaginary $\epsilon_2(\omega)$ and real $\epsilon_1(\omega)$ dielectric function of CdSe compound in WZ- and ZB- phase are calculated within time dependent density functional perturbation theory (TD-DFPT) using a Lanczos chain as illustrated in Fig. 4. The absorption coefficient and the loss function in terms of real and imaginary part of dielectric function is given by:

$$\beta(\omega) = \sqrt{2}\omega \left[\sqrt{\epsilon_1(\omega)^2 + \epsilon_2(\omega)^2} - \epsilon_1(\omega) \right]^{\frac{1}{2}}, \quad (3)$$

$$L(\omega) = \frac{\epsilon_2(\omega)}{\epsilon_1(\omega)^2 + \epsilon_2(\omega)^2}$$

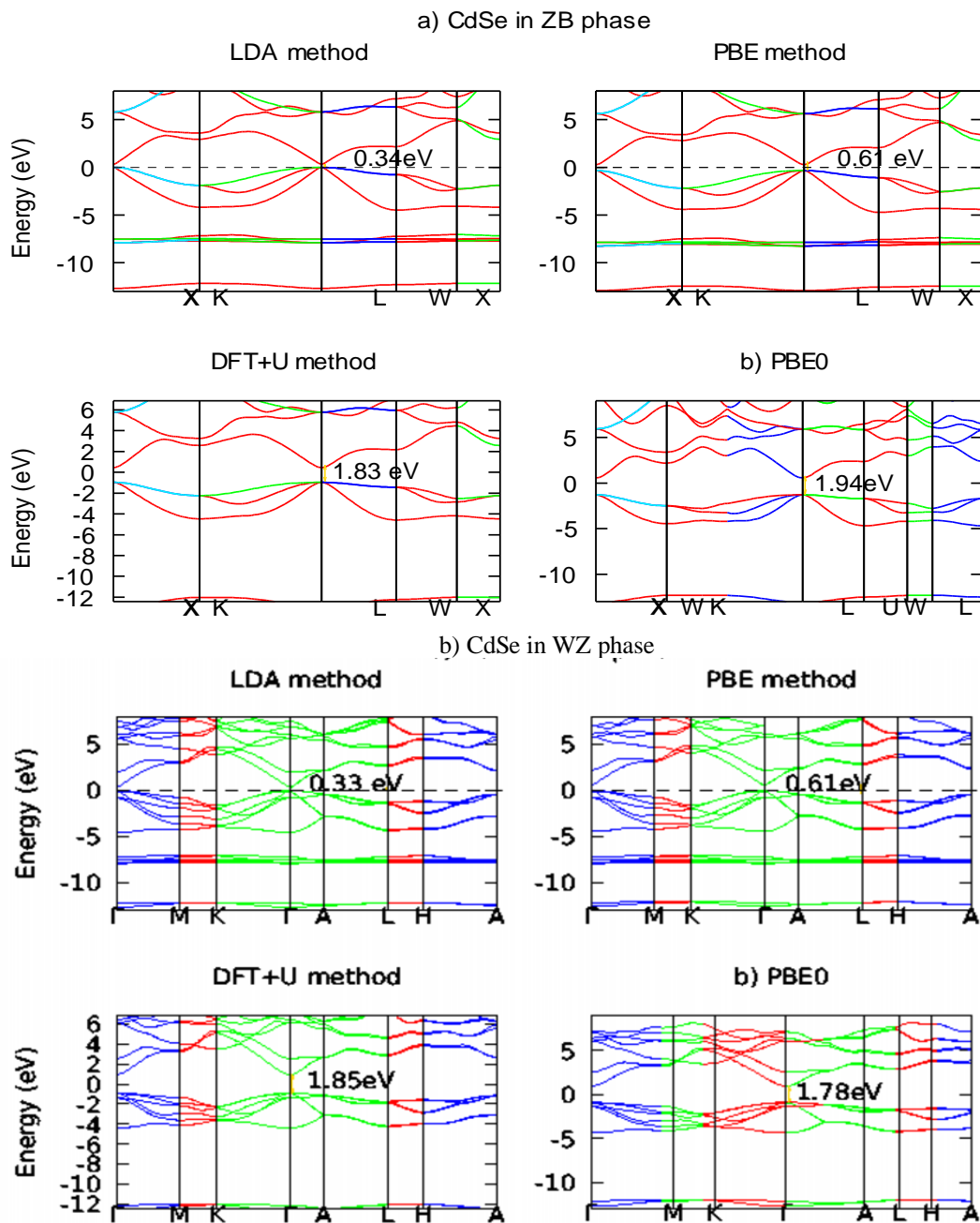
Many peaks are corresponding to different electronic transitions observed in the spectra of real and imaginary part of the dielectric function. The polarization effects and strength of dynamical screening are described by the real part of the dielectric function $\epsilon_1(\omega)$. However, the energy absorption as the result of charge excitation is related to the imaginary part of the dielectric function $\epsilon_2(\omega)$. The

peaks observed in the optical spectra are related to the transitions from the valence to conduction bands in the electronic energy band structure of high symmetry points in the Brillouin zone. Due to many body interactions and the random orientation of the transition dipole moments, the oscillatory trend is observed in the spectrum. The oscillatory trend in this

Table 2

Comparison of calculated band gap of CdSe and Experimental value.

Phase \ Methods	LDA	PBE	DFT+U	PBE0	Experiment
ZB	0.33	0.61	1.83	1.94	1.90 [33, 35]
WZ	0.37	0.65	1.85	1.76	1.80 [33]


Fig. 2. Band structure of CdSe along high symmetry points: a) in ZB phase b) WZ phase

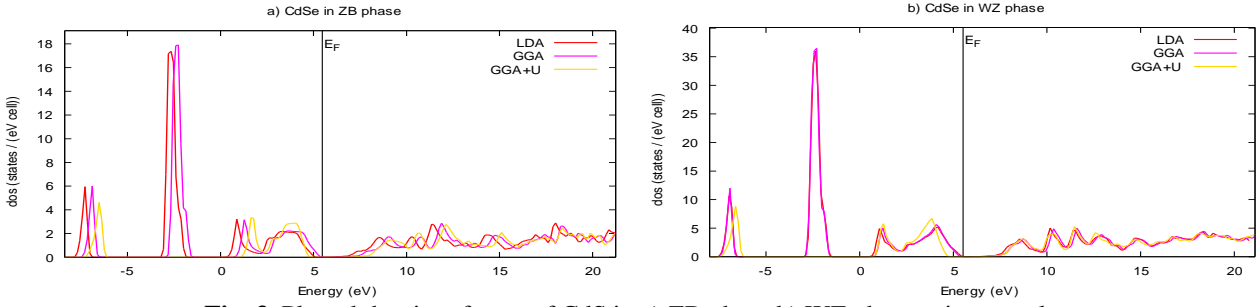


Fig. 3. Plotted density of state of CdS in a) ZB phase b) WZ phase using gnuplot.

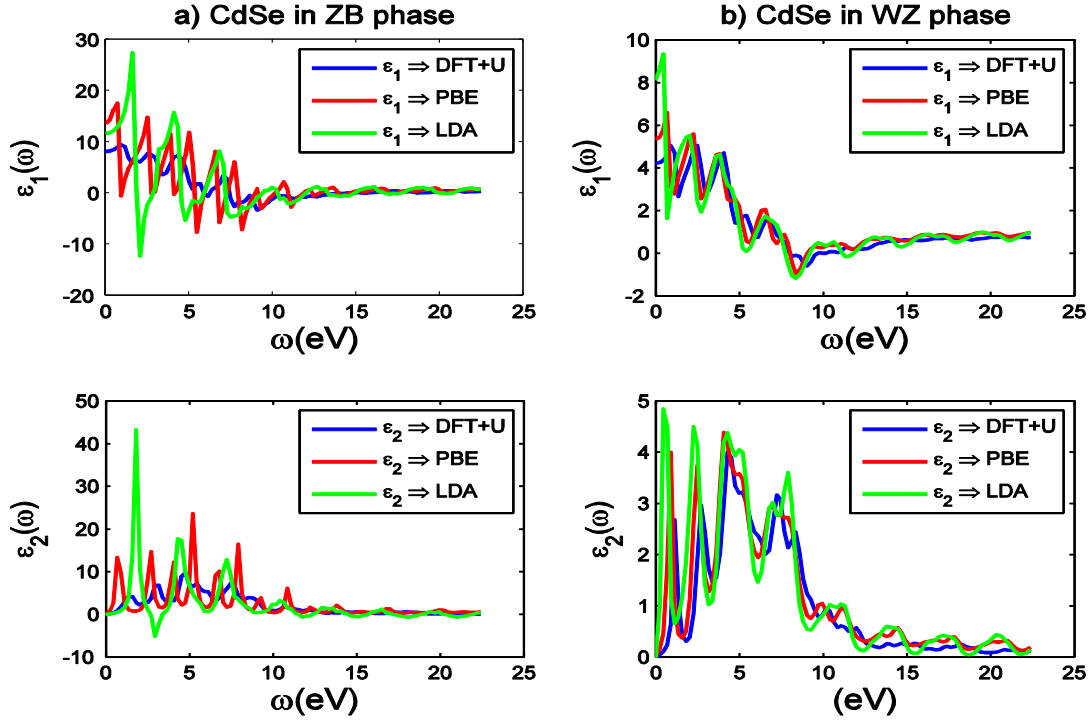


Fig. 4. Real and imaginary parts of dielectric function for (a) ZB-CdSe and (b) WZ-CdSe

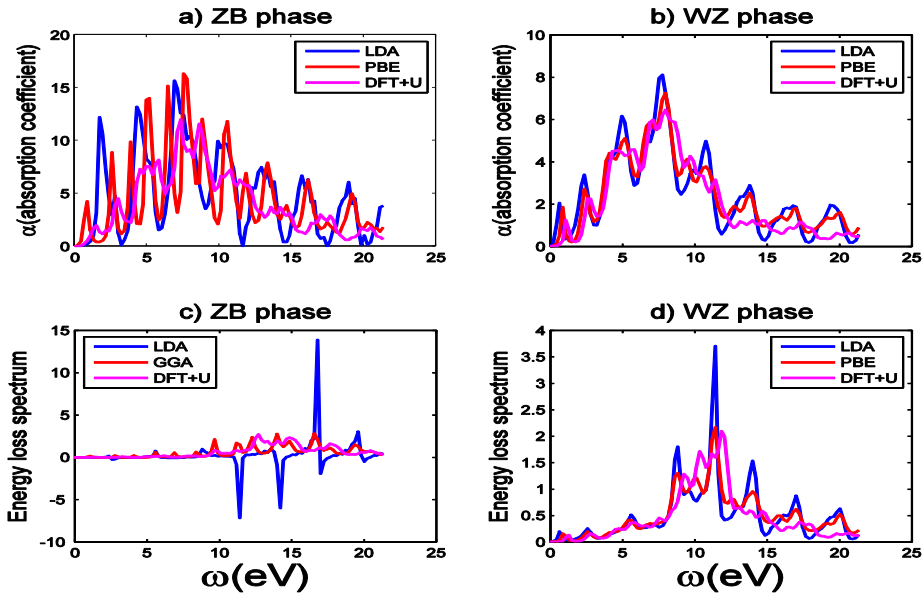


Fig. 5. Absorption Coefficients for CdSe (a) ZB-CdSe (b) WZ-CdSe and Energy loss spectrum for (a) ZB-CdSe (b) WZ-CdSe.

spectrum represents the presence of many body interactions and it is dependent upon strength of transition.

From Fig. 4a one can observe that the real part of dielectric function $\epsilon_1(\omega)$ of ZB-CdSe structure has maximum peak of 27.44 at photon energy of 1.5392 eV using LDA approximation. According to PBE approximation it has maxima at 17.6246 at photon energy of 0.6597 eV. For DFT+U approximation the maximum value is 9.5508 at photon energy of 0.8796 eV. Moreover, the values of the static dielectric constant $\epsilon_1(0)$ of ZB-CdSe is 11.7595, 13.7050 and 8.2099 for LDA, PBE and DFT+U approximations respectively. The experimental value of static dielectric constant of ZB CdSe is 8.61[43]. The static dielectric constant obtained using DFT + U approximation is in good agreement with the experimental value with a percentage error of 4.6 %.

As shown in Fig. 4b the real part of dielectric function $\epsilon_1(\omega)$ of WZ-CdSe structure has 9.341 for photon energy of 0.4398 eV, 6.5965 at photon energy of 0.6597 eV, and 5.0637 at photon energy of 2.4188 eV with respect to LDA, PBE and GGA +U approximations respectively. The static dielectric constant of WZ-CdSe is 8.1211, 5.3536 and 4.2133 using LDA, PBE and DFT+U approximations in that order. The experimental value of a static dielectric constant of WZ CdSe for parallel component is 10.1 [43]

The peak magnitudes of imaginary part of the dielectric function for ZB-CdSe is 43.3684 at photon energy of 1.7591 eV, 23.5075 at photon energy of 5.0575, and 9.7116 at photon energy of 4.6177 in accord with LDA, PBE and PBE +U approximations in that order. However, the peak values for WZ-CdSe are 4.84 at photon energy of 0.439eV, 3.9948 at photon energy of 0.8796 eV and 4.0028 at photon energy of 4.1779 eV using LDA, PBE and PBE+U approximations respectively.

The absorption coefficient and the energy loss function spectrum for ZB- and WZ-CdSe structure are determined from frequency dependent dielectric function using equation (3). The energy loss spectrum and absorption coefficient are demonstrated in Fig. 5.

The optical absorption spectrum of ZB- and WZ-CdSe based on LDA, PBE, and DFT+U approximations are demonstrated in Fig. 5a and 5b. The energy dependent spectra of absorption has a viable increasing and decreasing trend. Most of the peaks correspond to different electronic transitions from occupied to unoccupied band. Moreover, the oscillatory trend in these spectrums represents many body interactions. It is resulted from random orientation of the transition dipole moments with applied electromagnetic field. The maximum values of absorption coefficient are 15.6628, 16.3048 and 11.6307 for ZB-CdSe with respect to LDA and PBE and DFT + U approximations respectively. However, the maximum value of absorption coefficients for WZ-CdSe are 8.1307, 7.2510 and 6.4447 using LDA, PBE and DFT+U approximations in that order.

Fig. 5c and d describes the value of energy loss

determined using equation (3). The energy loss-spectrum is important for describing the energy loss of fast electrons passing through the -ZB or -WZ phase of CdSe. The peaks of $L(\omega)$ (5c and 5d) correspond to the rapid decrease in reflectance. The energy loss function $L(\omega)$ determines the loss of energy while traversing through the material. However, the absorption coefficient describes the transition of electrons from valence band to the conduction band.

Conclusion

The structural, electronic and optical properties of ZB- and WZ-CdSe are studied using density functional theory. The exchange correlation functional is approximated using LDA, GGA/PBE, GGA + U and PBE0. The values of lattice constants obtained using LDA, PBE, DFT + U and PBE0 approximations are in good agreement with experimental results. The band gap values of ZB CdSe obtained using LDA and PBE potential approximations are severely under estimated with percentage error of 82 % and 68 % respectively compared to the experimental value. Moreover, the band gap values of WZ CdSe with respect to LDA and PBE approximations are with percentage error of 79 % and 64 % when compared with experimental values. However, the band gap values determined using Hubbard correction and hybrid functions are in a very good agreement with the experimental values with percentage error of 3 % and 2 % respectively for both phases. In addition to the above parameters, the optical properties such as the real part $\epsilon_1(\omega)$ and; maginary part $\epsilon_2(\omega)$ of the dielectric function, static dielectric constant $\epsilon(0)$, the absorption coefficient and the energy loss function are studied as a function of photon energy. The real part of the dielectric function is related to the transmission of photons within the material. However, the imaginary part of the dielectric function describes the absorption coefficient. The energy loss function shows the lost energy while the electromagnetic wave traverses inside both phases of CdSe. The absorption coefficient describes the transition of electrons from valence band to the conduction band from different orbitals.

Acknowledgements

One of the authors Teshome Gerbaba expresses his thanks and appreciation to the Department of Physics, Wollega University for its material support in this study.

Edossa T.G. - PhD Candidate in Condensed Matter Physics, Lecturer of the Physics Department.
Woldemariam M.M. - PhD in Condensed Matter Physics, Associate Professor of Condensed Matter Physics.

- [2] A.L. Efros and M. Rosen, The electronic structure of semiconductor nano crystals, *Annu. Rev. Mater. Sci.* 30, 475 (2000) (<https://doi.org/10.1146/annurev.matsci.30.1.475>).
- [3] K.R. Murali, V. Swaminathan & D.C. Trivedi, *Solar Energy Materials & Solar Cells* 81(1), 11 (2004) (<https://doi.org/10.1016/j.solmat.2003.08.019>).
- [4] S.T. Bulbula. & H.W. Zeweldi, *Advances in Materials Science and Engineering* 2015, 1 (2015) (<https://doi.org/10.1155/2015/847693>).
- [5] A.S. Khomane, P.P. Hankare, *Journal of Alloys and Compounds*, 489(2), 605 (2010) (<https://doi.org/10.1016/j.jallcom.2009.09.122>).
- [6] S. Sharma and A.S. Verma, *Advanced Materials Research* 665, 302 (2013) (<https://doi.org/10.4028/www.scientific.net/AMR.665.302>).
- [7] M.A. Schreuder, K. Xiao, I.N. Ivanov, S.M. Weiss and S.J. Rosenthal, *Nano Lett.* 10, 573 (2010) (<https://doi.org/10.1021/nl903515g>).
- [8] M.C. Schlamp, X. Peng X and A.P. Alivisatos, *J. Appl. Phys.* 82, 5837 (1997) (<https://doi.org/10.1063/1.366452>).
- [9] M. Nirmal, B.O. Dabbousi, M.G. Bawendi, J.J. Macklin, J.K. Trautman, T.D. Harris and L.E. Brus, *Nature*, 383, 802 (1996) (<https://doi.org/10.1038/383802a0>).
- [10] D. Thomas, H.O. Le III, K.C. Santiago, et al., *Journal of nanomaterials* 2020, 1 (2020) (<https://doi.org/10.1155/2020/5056875>).
- [11] L. Qu and X. Peng, *J. Am. Chem. Soc.* 124(9), 2049 (2002) (<https://doi.org/10.1021/ja017002j>).
- [12] B. Sun, E. Marx and N.C. Greenham, *Nano Lett.* 3(7), 96 (2003) (<https://doi.org/10.1021/nl0342895>).
- [13] C.E. Hamilton, D.J. Flood and A.R. Barron, *Phys. Chem. Chem. Phys.* 15, 3930 (2013) (<https://doi.org/10.1039/C3CP50435B>).
- [14] V.A. Fedorov, V.A. Ganshin, & Yu.N. Korkishko, *Physica status solidi (a)*, 28 1 (1991) (<https://doi.org/10.1002/pssa.2211260133>).
- [15] Su-Huai Wei and S.B. Zhang, *Phy. Rev. B* 62, 6944 (2000) (<https://doi.org/10.1103/PhysRevB.62.6944>).
- [16] K.O. Magnusson, G. Neuhold, K. Horn and D.A. Evans, *Phy. Rev. B* 57, 8945 (1998) (<https://doi.org/10.1103/PhysRevB.57.8945>).
- [17] E. Deligoz, K. Colakoglu and Y. Ciftci, *Physica B* 373, 124 (2006) (<https://doi.org/10.1016/j.physb.2005.11.099>).
- [18] D. Singh, A.K. Bandyopadhyay, M. Rajagopalan, P.Ch. Sahu, M. Yousuf and K. Govinda Rajan, *Solid state Commun* 109(5), 339 (1999) ([https://doi.org/10.1016/S0038-1098\(98\)00552-3](https://doi.org/10.1016/S0038-1098(98)00552-3)).
- [19] H. Eschrig, *The Fundamentals of Density Functional Theory* (Springer Vieweg, 1st edn, 1 (1996). (<https://doi.org/10.1007/978-3-322-97620-8>).
- [20] Li, Bo., *Density-Functional Theory and Quantum Chemistry Studies on dry and wet NaCl (001)*, PhD Thesis, 1 (2008) (<http://hdl.handle.net/11858/00-001M-0000-0010-FB4E-2>).
- [21] K. Deguchi, Y. Takano, and Y. Mizuguchi, *Science and Technology of Advanced materials* 13(5), 1 (2012) (<https://doi.org/10.1088/1468-6996/13/5/054303>).
- [22] A.S.Z. Lahewil, Y. Al-Douri, U. Hashim & N.M. Ahmed, *Procedia Engineering* 53, 217 (2013) (<https://doi.org/10.1016/j.proeng.2013.02.029>).
- [23] Lev I. Berger, *Semiconductor materials*, (CRC Press, France 1st edn., France, 1996) (ISBN 0-8493-8912-7) (<https://doi.org/10.1103/PhysRevLett.77.3865>).
- [24] P. Giannozzi et al, *J. Phys: Condens. Matter.* 9(46), 1 (2017) (<https://doi.org/10.1088/1361-648X/aa8f79>).
- [25] P. Giannozzi et al, *J. Phys.: Condens. Matter.* 21(39) 1 (2009) (<https://doi.org/10.1088/0953-8984/21/39/395502>).
- [26] J.P. Perdew and A. Zunger, *Phys. Rev. B* 23, 5048 (1981) (<https://doi.org/10.1103/PhysRevB.23.5048>).
- [27] J.P. Perdew, K. Burke, and M. Ernzerhov, *Phys. Rev. Lett.* 77 3865 (1996). (<https://doi.org/10.1103/PhysRevLett.77.3865>).
- [28] S.L. Dudarev, G.A. Dudarev, S.Y. Savrasov, et al., *Phys Rev. B*, 57(3), 1505 (1998) (<https://doi.org/10.1103/PhysRevLett.77.3865>).
- [29] D. Fritch, B.J. Moorgan and A. Walsh, *Nanoscale Research Letters* 12(19), 1 (2017) (<https://doi.org/10.1186/s11671-016-1779-9>).
- [30] K.F. Garrity, J.W. Bennett, K.M. Rabe, D. Vanderbilt, *Computational material science* 81, 446 (2014) (<http://dx.doi.org/10.1016/j.commatsci.2013.08.053>).
- [31] M. Topsakal, R.M. Wentzcovitch, *Computational material science*, 95, 263 (2014) (<http://dx.doi.org/10.1016/j.commatsci.2014.07.030>).
- [32] Monkhorst, Hendrik J., and James D. Pack, *Phys. Rev. B*, 13(12), 5188 (1976) (<https://doi.org/10.1103/PhysRevB.13.5188>).
- [33] P. Gopal et al, *Phys. Rev. B* 91, 2452021 (2015) (<https://doi.org/10.1103/PhysRevB.91.245202>).
- [34] D. Prasad P.S., B.K. Sarkar, *Mechanics, Materials Science & Engineering Journal*, Magnolithe, 9 (2017) ISSN 2412-5954 (<https://doi.org/10.2412/mmse.32.38.817>).
- [35] E. Deligoz, K. Colakoglu and Y. Ciftci, *Physica B* 373 (2006), 124 (2005) (<https://doi.org/10.1016/j.physb.2005.11.099>).

- [36] O. Zakharov, A. Rubio, & M. L. Cohen, Physical Review B, 51(8) 4926 (1995) (<https://doi.org/10.1103/PhysRevB.51.4926>).
- [37] O. Madelung, Semiconductors: Data Hand book (Springer, New York, NY, USA, 2004).
- [38] K. Capelle, Brazilian Journal of Physics 36(4), 1 (2006) (<https://doi.org/10.1590/S0103-97332006000700035>).
- [39] S. Thirumavalan, K. Mani, and S. Sresh, Chalcogenide Letters 12(5), 237 (2015) (ISSN 1584-8663).
- [40] N.A. Noor, et al., Journal of Alloys and Compounds 507, 356 (2010) (<https://doi.org/10.1016/j.jallcom.2010.07.197>).
- [41] N. Ullah, G. Murtaza, R. Khenata, K.M. Wong & Z.A. Alahmed, A multinational journal 87(6), 571 (2013) (<https://doi.org/10.1080/01411594.2014.886110>).
- [42] J.M. Carcione, F. Cavalline, J. Ba, et al., Rheol Acta, 58, 28, (2019) (<https://doi.org/10.1007/s00397-018-1119-3>).
- [43] C. Janowitz, et al., Phys. Rev. B 50, 2181 (1994) (<https://doi.org/10.1103/PhysRevB.50.2181>).

Т.Г. Едосса¹, М.М. Волдемаріам²

Електронні, структурні та оптичні властивості селеніду кадмію (CdSe) у структурі цинкової обманки та в'юрциту, використовуючи теорію функціоналу густини та поправки Хаббарда

¹Коледж природничих та обчислювальних наук, Університет Воллеги, Воллега, Ефіопія. teshgerb@gmail.com

²Коледж природничих наук, Університет Джимми, Джимма, Ефіопія. memberu.mengesha@ju.edu.et

Структури селеніду кадмію (CdSe) типу цинкової обманки (ZB) та в'юрциту (WZ) визначено, використовуючи теорію функціоналу густини у межах наближення локальної густини (LDA), узагальненого наближення градієнта (GGA), корекції Хаббарда (GGA + U) та наближення гібридного функціоналу (PBE0 або HSE06). Використовуючи псевдопотенціал плоских хвиль із перших принципів отримано релаксаційні положення атомів CdSe у структурі ZB та WZ на основі методу мінімізації загальної енергії та сил за наближенням Геллмана і Фейнмана. Перевірка на збіжність загальної енергії щодо енергії відсікання та k-точки проводили для забезпечення необхідної точності розрахунку. Розраховано константи рівноважних сталих ґратки та об'єм елементарної комірки CdSe для обох фаз. Отримане значення порівнюється із експериментальними значеннями. Крім того, ширина забороненої зони CdSe аналізується за допомогою DFT в межах LDA, GGA, DFT + U та PBE0 для наближення невідомого обмінного кореляційного функціоналу. Значення ширини забороненої зони, отримані з використанням LDA та GGA, подекуди недооцінені через їх погану апроксимацію обмінно-кореляційного потенціалу. Цю проблему було покращено за допомогою використання проектора псевдопотенціалу доповненої хвилі в рамках корекції Хаббарда (GGA + U) та гібридного функціонального наближення. Оптичні властивості: виконано дослідження комплексних та дійсних частин діелектричної функції, спектру втрат енергії та коефіцієнту поглинання CdSe як у фазі ZB, так і у фазі WZ.

Ключові слова: селенід кадмію, ДФТ, рівноважна стала ґратки, зонна структура, оптичні властивості.